Sustainability **2014**, *6*, 5300-5310; doi:10.3390/su6085300

OPEN ACCESS

sustainability

ISSN 2071-1050

www.mdpi.com/journal/sustainability

Article

Information Extraction of High-Resolution Remotely Sensed Image Based on Multiresolution Segmentation

Peng Shao, Guodong Yang, Xuefeng Niu *, Xuqing Zhang, Fulei Zhan and Tianqi Tang

College of Geo-exploration Science and Technology, Jilin University, Changchun 130026, China; E-Mails: 15948774363@163.com (P.S.); ygd@jlu.edu.cn (G.Y.); zxq@jlu.edu.cn (X.Z.); zfl2014zfl@163.com (F.Z.); ttq2014ttq@163.com (T.T.)

* Author to whom correspondence should be addressed; E-Mail: niuxf@jlu.edu.cn; Tel.: +86-138-4301-7218.

Received: 29 May 2014; in revised form: 25 July 2014 / Accepted: 28 July 2014 / Published: 14 August 2014

Abstract: The principle of multiresolution segmentation was represented in detail in this study, and the canny algorithm was applied for edge-detection of a remotely sensed image based on this principle. The target image was divided into regions based on object-oriented multiresolution segmentation and edge-detection. Furthermore, object hierarchy was created, and a series of features (water bodies, vegetation, roads, residential areas, bare land and other information) were extracted by the spectral and geometrical features. The results indicate that the edge-detection has a positive effect on multiresolution segmentation, and overall accuracy of information extraction reaches to 94.6% by the confusion matrix.

Keywords: edge-detection; object-oriented; multiresolution segmentation; spectral features; geometrical features; confusion matrix

1. Introduction

In recent years, high-resolution satellite remote sensing technology has been developed rapidly. The high-resolution satellite images include spectral, geometry, space, texture and other information. Traditional pixel-based information extraction methods only use spectral information. It is difficult to overcome the widespread phenomenon, in which the same body usually has a different spectrum, and different bodies have the same spectrum in the image. Therefore, information extraction technology

which is suitable for high-resolution remotely sensed image based on object-oriented multiresolution segmentation has become inevitable.

Since 2000, more and more scholars have attended to the methods of information extraction based on object-oriented multiresolution segmentation. Winhauck used this method and the traditional visual interpretation method to process SPOT data respectively, and the results showed that the classification accuracy is better than the latter [1]. Hofmann improved the classification accuracy of the residential areas in IKONOS images by combining spectrum of the object, texture and shape with the background information [2–6]. Benz considers that object-oriented extraction method can improve the efficiency of automatic extraction and has development potential in high-resolution remotely sensed images [7–10]. W. Myint used the pixel-based extraction method and the object-oriented multiresolution segmentation method to extract QuickBird satellite images respectively. The results showed that the former accuracy is only 63.33%, while the latter is up to 90.04% [11–13]. Du Fenglan discussed the application of this method in the information extraction of IKONOS image [14,15]. Sun Xiaoxia used object-oriented method to extract rivers and roads from IKONOS images [16]. Zhou Chunyan took the Object-oriented technique to extract high-resolution remotely sensed images for land-use classification, which eliminated the salt and pepper phenomenon of the traditional method, and consequently improved the overall accuracy compared to the method of maximum likelihood [17]. Tao Chao took grading extraction for the city buildings based on this method [18]. Chen Jie studied the extraction of object-oriented multiresolution segmentation for multispectral image and the method which is based on rough sets and supports vector machine .In summary, the object-oriented extraction method based on the multiresolution segmentation breaks through the limitations of traditional methods, and achieved excellent results. There is potential for further study in the area of the information extraction of high-resolution images.

In this study, Korea resources an area of ZY-3 satellite image data as an example to study the information extraction method based on multiresolution segmentation. The canny algorithm is used to detect the edge of the image first, and the results will be assisted in the multiresolution segmentation of original image. The spectral characteristics and the geometry features will be used to extract ground object information.

2. Principle and Methods

2.1. Multiresolution Segmentation

Image segmentation is the process of dividing image area into non-overlapping and non-empty regions. It has the same or similar features in a region, and the same or similar features can be gray-scale, color, texture, and other features. The algorithm of region merging is used in multiresolution segmentation. Firstly, pixels will be combined into smaller image objects, and then smaller image objects will be merged into larger polygon objects. The smallest heterogeneity of the polygon objects maximally reduces the whole image objects' average heterogeneity under the given segmentation threshold. Scale factor, spectral heterogeneity and shape heterogeneity will be taken into account in the multiresolution segmentation. Scale parameter is used to measure the maximum value of heterogeneous change as two objects were merged, and the square of the value is the condition to stop

the merger. The objects will be continue to be merged when the value of the heterogeneity is less than the square of the scale parameter, otherwise, the process will be stopped. The larger the scale is, the larger the object is, and vice versa. The shape heterogeneity has two parameters: smoothness h_{sm} and compactness h_{cm}. The smoothness represents the smooth degree of the object obtained in the process, and the compactness ensures the combined object more compact. The measurement principles of spectral heterogeneity and shape heterogeneity are as follows:

Combination of the two measurement criteria is shown in Formula (1):

$$f = \omega \cdot h_{color} + (1-\omega) \cdot h_{shape} \tag{1}$$

where ω = spectral heterogeneity weights, its value is 0 to 1.

The spectral parameter heterogeneity is shown in Formula (2):

$$h_{color} = \sum_c \omega_c \cdot \sigma_c \tag{2}$$

where c = number of bands

ω_c =Layer weights

σ_c = standard value of the spectral bands

If the standard and the area of two adjacent regions are designated as σ_c^{o1}, n_{o1}, σ_c^{o2}, n_{o2}, The weight of the band is ω_c, then the combined area n_{merge} and variance σ_c^{merge} of the region are shown in Formula (3):

$$h_{color} = \sum_c \omega_c (n_{merge} \cdot \sigma_{merge} - (n_{o1} \cdot \sigma_c^{o1} + n_{o2} \cdot \sigma_c^{o2})) \tag{3}$$

The parameter of shape heterogeneity is shown in (4):

$$h_{sm} = \frac{l}{b}, h_{cm} = \frac{l}{\sqrt{n}} \tag{4}$$

where l = perimeter of the area

b = the perimeter of the minimum bounding rectangle

n = the area of minimum bounding rectangle

If l and b of the two adjacent regions are $l_{o1}, b_{o1}, l_{o2}, b_{02}$ respectively, then the shape parameters h_{smooth}, $h_{compact}$ are shown as follows:

$$h_{smooth} = n_{merge} \cdot \frac{l_{merge}}{b_{merge}} - (n_{o1} \cdot \frac{l_{o1}}{b_{o1}} + n_{o2} \cdot \frac{l_{o2}}{b_{02}}) \tag{5}$$

$$h_{compact} = n_{merge} \cdot \frac{l_{merge}}{\sqrt{n_{merge}}} - (n_{o1} \cdot \frac{l_{o1}}{\sqrt{n_{o1}}} + n_{o2} \cdot \frac{l_{o2}}{\sqrt{n_{o2}}}) \tag{6}$$

Final shape heterogeneity is as follows:

$$h_{shape} = \omega_{compact} \cdot h_{compact} + (1-\omega_{compact}) \cdot h_{smooth} \tag{7}$$

Generally, spectral information is the most important, and the factor weights of the spectrum should be designated larger as soon as possible. The shape factor makes the generated object with good

smoothness and compactness, and improves the integrity of the object. The stop condition of image segmentation is determined by the scale parameter, which depended on the interest information.

2.2. Information Extraction

In the process of extracting information based on the multiresolution segmentation, the object layers are created first, and then features are extracted by considering the spectrum, shape, size, texture, and topology and context characteristics of the object. The smallest unit of image is not a single pixel, but the object obtained by segmentation, and the subsequent information extraction is based on it. The descriptions of the common characteristics are as follows.

(1) Spectral features

The common spectral features include the mean value, brightness and standard deviation. The mean value is obtained by calculating all values of pixels of the image object layers. Brightness refers to the sum of the layers average value divided by the number of the image object layers. The Standard deviation is calculated by all pixels in one object layer.

(2) Geometrical features

Geometric features are based on the spatial distribution statistics of pixels constituting the image object. Covariance matrix can be used as a core tool for statistical treatment. If X and Y are constituted the image object x and y coordinates respectively, then the covariance matrix can be described as follows:

$$\mathrm{A} = \begin{bmatrix} Var(X) & Cov(XY) \\ Cov(XY) & Vor(Y) \end{bmatrix} \tag{8}$$

The Geometric features of the object can also be provided approximately by the length, width, area and filling degree of the bounding box. The main geometrical features include length, width, area, length/width, density, shape index. The area of a single pixel is 1. The area of an object is its number of pixels. The length and width are the eigenvalues of covariance matrix, and can also be approximated instead of the object's bounding box. The aspect ratio is the ratio of the covariance's eigenvalues, and calculated approximately by the bounding box, and the lowest value will be used as the characteristic value. The Density describes the compactness of the image object, the more the object tends to square, the greater the density. The Shape index describes the smoothness of the boundary of the object, the more broken image object, the greater its value. It is described by the boundary length (sum of an image object and the other co-owner of the image boundary or edge of the entire image) of one object divided by the square root of its area four times.

3. Information Extraction

3.1. Study Area and Data Sources

The experimental data is a regional resource Korea ZY-3 image (Figure 1). The satellite launches on January 9, 2012, its panchromatic resolution is 2.1 m, and multispectral (blue, green, red) resolution is 5.8 m, the coordinate system is WGS_1984. The region is located in the border, and the main information is complete, including water bodies, vegetation, residential areas, roads, bare land, *etc.*

Figure 1. Original image.

3.2. Multiresolution Segmentation

In this study we did not only divide the original image into objects, but the edge information was used for the multiresolution segmentation. Because Canny Operator has good detection (the algorithm should mark as many real edges in the image as possible), good localization (edges marked should be as close as possible to the edge in the real image) and minimal response (a given edge in the image should only be marked once, and where possible, image noise should not create false edges), this test uses a canny operator to detect the edge of image layer 3. The result is shown in Figure 2. It can be seen in the figure that the edge is obvious, and it is advantageous to the subsequent multiresolution segmentation, especially for extracting road extraction. The weights of canny, R, G, and B layer were set to 5, 1, 1, 1 respectively, scale parameter was set to 30, the shape heterogeneous degree was 0.1 (the spectral heterogeneity degree was 0.9), and compactness and smoothness both were 0.5. Features of the object were not broken in this scale, and all kinds of features were integral. This is advantageous to the subsequent information extraction. Then the results were compared with the results without using edge in segmentation. As shown in Figure 3, it can be seen that the objects, with the assistance of edge information, were more integral under the same parameters, and this is conducive to the subsequent information extraction.

Figure 2. Edge detection (partial).

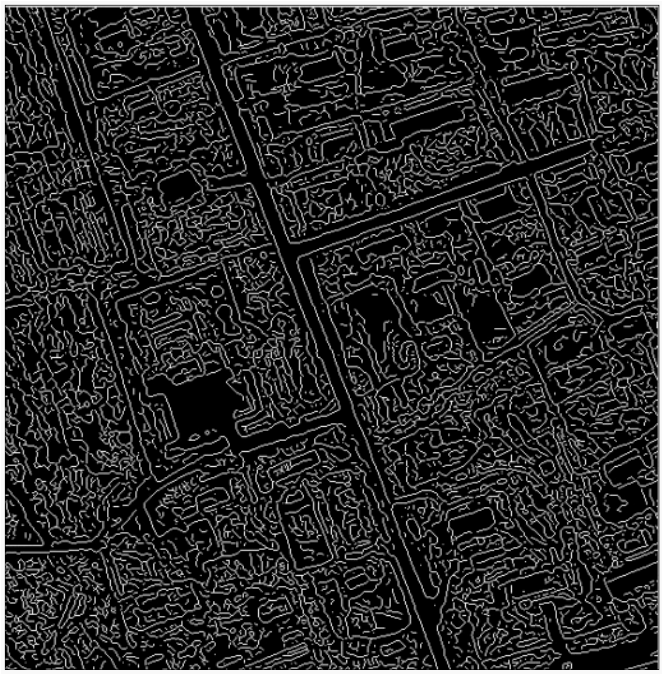

Figure 3. Multiresoulution segmentation results contrast under the same scale (**left**: with edge information and **right**: without edge information).

3.3. Main Features Extraction

3.3.1. Water Body Extraction

As the water in the image is on the performance of dark tones, the band means, brightness, and other spectral feature can be used in extraction, the mean of layer 3 and the custom feature B (as shown in Formula (8)) were used.

$$\frac{MeanLayer2 + MeanLayer3 - 2 \cdot MeanLayer1}{MeanLayer2 + MeanLayer3 + 2 \cdot MeanLayer1} \quad (9)$$

3.3.2. Vegetation Extraction

Since the experimental data has no near-infrared band, The NDVI cannot be used to extract vegetation information; thus, the mean of Layer 3 and custom feature green band ratio G (as shown in Formula (9)) were used.

$$\frac{MeanLayer2}{MeanLayer3 + MeanLayer2 + MeanLayer1} \quad (10)$$

3.3.3. Road Extraction

Spectrum characteristics of road and resident are similar, so it is difficult to identify them by the spectral feature. The roads on the image are seen as long strips, so the object's shape index, compactness, density and aspect ratio were used to extract road information.

3.3.4. Residential Areas Extraction

The reflectance of residential areas is high, and buildings are usually more or less rectangular, so the brightness, shape index and rectangular fit will be used to extract residential areas.

3.3.5. Bare Land and Other Extraction

Because the reflectance of bare land and other information is high, the brightness and the custom feature B are used to extract bare land and other information.

Finally, the features had been misclassified were corrected through the human-computer interaction function. The vector data was exported and added to the original image to make comparative analysis. The rules of information extraction are shown in Table 1 and the results are shown in Figures 4 and 5.

Table 1. The rule of Information extraction table.

Information Category	Extraction Rules
Water	B is more than0.04, Layer 3 is less than 84
Vegetation	G is more than0.34, Layer 3 is less than 80
Road	Shape index is more than7, Compactness is more than 6, density is less than1, Length/width is more than 6
Residential area	Brightness is more than140,Shape index is more than 5, rectangular fit is more than 0.5
Bare Land	Brightness more is than120, B is more than −0.03

Figure 4. Results of information extraction.

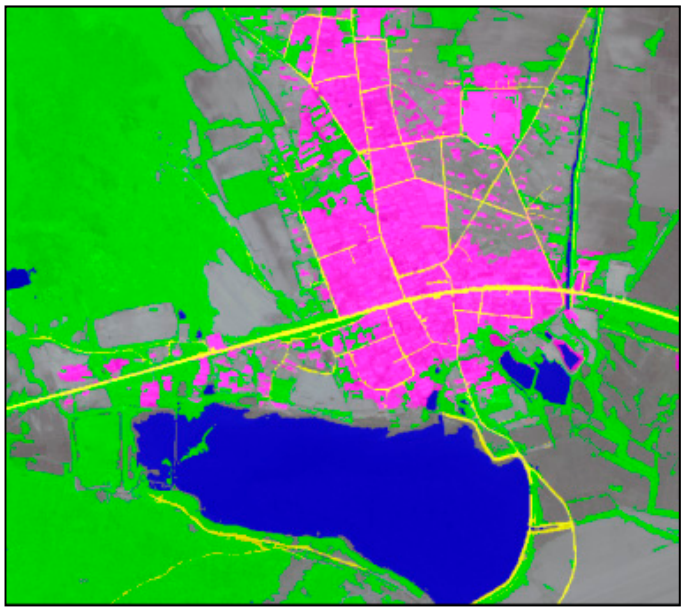

Figure 5. The vector.

3.4. Accuracy Analysis

The confusion matrix was used to make an accuracy evaluation for the result of the information extraction. The confusion matrix mainly is used to compare the classification results and the actual measured values in the image accuracy evaluation. The accuracy of the classification results can be displayed in a confusion matrix. The confusion matrix is calculated by the position of each pixel and classification of the corresponding image. Each column of the confusion matrix represents the actual measured information, and each row represents the classified information of remote sensing data. The higher the diagonal elements are, the higher the extraction precision is, and vice versa. This experiment

has selected sample areas from the original image to calculate the confusion matrix, and the results are shown in Table 2, and the overall accuracy reaches to 0.946.

Table 2. Accuracy Analysis.

Use class	Water	Vegetation	Road	Bare Land	Residential	Sum
Water	97	0	0	0	0	97
Vegetation	0	177	1	11	2	191
Road	0	0	78	0	1	79
Bare Land	0	0	2	171	0	173
Residential	0	0	4	7	126	133
Sum	97	177	85	189	127	
Accuracy						
Producer	1	1	0.918	0.905	0.913	
User	1	0.926	0.987	0.94	0.92	
Kappa	1	1	0.907	0.87	0.891	
Totals						
Overall Accuracy				0.946		
Kappa				0.931		

4. Conclusions

The ZY-3 image of North Korea was used in this study. The canny algorithm was taken into image edge-detection to improve the effect of multiresolution segmentation. Taking advantage of edge-detection results in multiresolution segmentation made a positive effect on extracting information. The noises were eliminated and the local singularity problem and pepper-salt phenomenon were solved by combining adjacent pixels into the same object with multiresolution segmentation. After repeated experiments, we obtained the main object extracting parameter settings (water: B is more than 0.04, layer is less than 84; vegetation: G is more than 0.34, layer 3 is less than 80; roads: compactness is more than 6, density is less than 1, length/width is more than 6; residential area: brightness is more than 140, shape index is more than 5, rectangular fit is more than 0.5; bare land: brightness is more than 120, B is more than −0.03). The overall accuracy reaches 94.6%. In brief, information extraction based on the method of multiresolution segmentation simulates the human brain's cognitive process, which makes the accuracy of automatic information extraction as close as possible to the accuracy of the human eye's recognition (in fact, the accuracy of the former is less than or equal to the latter). The spectrum geometry and texture information of images are taken into account, and the extraction results on the high resolution remotely sensed image are significant.

Acknowledgments

This study was supported by the National Science and Technology Support Program "Digital Peripheral Geopolitical Environment Construction and key Technology Research" project. In addition, we wish to express our gratitude to Prof Chen Jun, the National Basic Geographic Information Center, and other colleagues in the subject group.

Author Contributions

Guodong Yang, Xuefeng Niu and Xuqing Zhang designed research, Tianqi Tang inquiried documents and information in this period. Fulei Zhan and Peng Shao performed research and analyzed the data. Peng Shao wrote the paper. All authors read and approved the final manuscript.

Conflicts of Interest

The authors declare no conflict of interest.

References

1. Willhauek, G. Comparison of object oriented classification techniques and standard image analysis for the use of change detection between SPOT multispectral satellite images and aerial photos. In Proceedings of XIX ISPRS Congress, Amsterdam, The Netherlands, 2000; pp. 35–42.
2. Hofmann, P. Detecting informal settlements from IKONOS data using methods of object oriented image analysis-an example from Cape Town (South Africa). Available online: http://www.ecognition.com/sites/default/files/395_hofmann.pdf (accessed on 29 May 2014).
3. Gong, P.; Li, X.; Xu, B. Interpretation theory and application method development for information extraction from high resolution remotely sensed data. *J. Remote Sens. Beijing* **2006**, *10*, 1–5.
4. Marangoz, A.M.; Oruc, M.; Buyuksalih, G. Object-oriented image analysis and semantic network for extracting the roads and building s from IKONOS pan-sharpened images. In Proceedings of the XXth Congress of International Society for Photogrammetry and Remote Sensing, Istanbul, Turkey, 2004; pp. 12–23.
5. Cheng, L.; Gong, J. Building Boundary Extraction Using Very High Resolution Images and Lidar. *Acta Geodaetica et Cartographica Sinica* **2008**, *37*, 391–393.
6. Im, J.; Jensen, J.R.; Tullis, J.A. Object-based change detection using correlation image analysis and image segmentation. *Int. J. Rem. Sens.* **2008**, *29*, 399–423.
7. Benz, U.C.; Hofmann, P.; Hofmann, P.; Willhauek, G. Mufti-resolution object-oriented fuzzy analysis of remote sensing data for GIS-ready information. *P&RS* **2004**, *58*, 239–258.
8. Baatz, M.; Schäpe, A. Multiresolution segmentation: An optimization approach for high quality multi-scale image segmentation. In *Angewandte. Geographische. Informationsverarbeitung XII*; Wichmann Verlag: Karlsruhe, Germany, 2000; pp. 12–23**.**
9. Zheng, J.; Shi, Y.; Qin, Y. Building Extraction from High Resolution Satellite Imagery Based on Multi-Scale Image Segmentation and Model Matching. In Proceedings of International Workshop on Earth Observation and Remote Sensing Applications, Beijing, China, 2008; pp. 1–7.
10. Mueller, M.; Segl, K.; Kaufmann, H. Edge-and region-based segmentation technique for the extraction of large, man-made objects in high-resolution satellite imagery. *Pattern Recogn.* **2004**, *37*, 1619–1628.
11. Myint, S.W.; Gober, P.; Brazel, A.; Grossman-Clarke, S.; Weng, Q. Per-pixel *vs.* object-based classification of urban land cover extraction using high spatial resolution imagery. *Remote. Sens. Environ.* **2011**, *115*, 1145–1161.

12. Herold, M.; Scepan, J.; Müller, A.; Günther, S. Object-oriented mapping and analysis of urban land use/cover using IKONOS data. In Proceedings of 22nd Earsel Symposium Geoinformation for European-Wide Integration, Prague, Czech Republic, 2002; pp. 4–6.
13. Baatz, M.; Schäpe, A. Object-oriented and multi-scale image analysis in semantic networks. In Proceedings of 2nd International symposium: Operationalization of remote sensing, Enschede, The Netherlands, 1999; pp. 16–20.
14. Du, F.; Tian, Q.; Xia, X. Object-oriented feature classification analysis and evaluation. *J. Remote. Sens. Tech. Appl.* **2004**, *19*, 20–24.
15. Stow, D.; Lopez, A.; Lippitt, C.; Hinton, S; Weeks, J. Object-based classification of residential land use within Accra, Ghana based on QuickBird satellite data. *Int. J. Rem. Sens.* **2007**, *28*, 5167–5173.
16. Sun, X.; Zhang, J.; Liu, Z. Using the object-oriented classification method from IKONOS panchromatic images to extract the rivers and roads. *Sci. Surv. Mapp.* **2006**, *31*, 62–63.
17. Zhou, C.; Wang, P.; Zhang, Z. Based on object oriented city coin land use classification information extraction technology. *Remote Sens. Tech. Appl.* **2008**, *23*, 31–35.
18. Tao, C.; Tan, Y.; Cai, H. Object-oriented high-resolution remote sensing image of city building hierarchical extraction method. *J. Surv. Mapp.* **2010**, *39*, 39–45.